Environmental and Experimental Botany 221 (2024) 105748

Contents lists available at ScienceDirect

Environmental and Experimental Botany

journal homepage: www.elsevier.com/locate/envexpbot

Research paper

Rice OBF binding protein 4 (OsOBP4) participates in flowering and regulates salt stress tolerance in *Arabidopsis*

Bello Hassan Jakada [a,1], Chutarat Punchkhon [a,1], Achmad Syarifudin [a], Triono Bagus Saputro [a], Teerapong Buaboocha [b,c], Supachitra Chadchawan [a,b,*]

[a] Center of Excellence in Environmental and Plant Physiology, Department of Botany, Faculty of Science, Chulalongkorn University, Bangkok, Thailand
[b] Omics Science and Bioinformatics Center, Faculty of Science, Chulalongkorn University, Bangkok, Thailand
[c] Molecular Crop Research Unit, Department of Biochemistry, Faculty of Science, Chulalongkorn University, Bangkok, Thailand

ARTICLE INFO

Keywords:
chlorophyll fluorescence
DOF family
flowering
OsOBP4
root development
stress tolerance

ABSTRACT

DNA-binding with one finger (DOF) transcription factors (TFs) play an important role in gene regulation for the proper growth and development of plants. Ocs-element binding factor (OBF) binding protein 4 (OBP4), an essential member of the DOF TF family, regulates flowering and abiotic stress. However, the functions of OBP4 in rice remain obscure, which limits its potential use in molecular breeding. In this study, rice *OBP4* (*OsOBP4*) was functionally characterized and its role in flowering and abiotic stress was verified. Phylogenetic analysis revealed that OsOBP4 is homologous to OBP4 in *Arabidopsis*. *OsOBP4* is modulated by salt, osmotic, and abscisic acid (ABA) stresses. Additionally, ectopic expression of *OsOBP4* complements the phenotype of the *Atobp4* mutation by enhancing root development and protecting the photosynthesis system. Under salt stress and short-day conditions, *OsOBP4* regulated floral development by interacting with AGL7, the upstream component for floral meristem initiation. These results provide evidence for the role of *OsOBP4* in multiple responses to salt stress and suggest that *OsOBP4* could be used as a potential candidate gene to improve tolerance to salt stress.

1. Introduction

Climate change is a major cause of environmental stress, which negatively affects the plant life cycle and productivity. It aggravates biotic and abiotic stresses and substantially affects plant sustainability and geographical distribution, thus posing a major threat to food security (Zhu, 2016; Pandey et al., 2017; Aslam et al., 2020; Park et al., 2022). Salinity damages approximately 20% of the irrigated land globally, and if current scenarios prevail, this value may rise to 50% (Nedjimi, 2011; Singh et al., 2020). The phenotypes displayed by plants in response to these stressors include delayed germination, reduced and deformed root growth, chlorosis, senescence, necrotic lesions, reduced leaf size, reduced stomatal number and size, wilting, and subsequent premature death (Meena et al., 2017; Singh et al., 2021). The world population is expected to grow beyond 9 billion by 2050 (Rose et al., 2016; Bailey-Serres et al., 2019; Aslam et al., 2022). Thus, an increase in food products such as rice is necessary to feed the rapidly growing world population.

Rice (*Oryza sativa* L.) is an essential crop and a staple food in many countries around the world (Bhatt et al., 2020; Muthuramalingam et al., 2022). Biotic and abiotic stresses resulting from climate change are responsible for reduced rice productivity in many regions worldwide (Verma et al., 2016; Bailey-Serres et al., 2019; Tang et al., 2020; Kojonna et al., 2022; Xu et al., 2022). To mitigate the effects of environmental stress, many pathways in plants are induced to produce and activate secondary signaling molecules in response to biotic and abiotic stresses.

Thailand is one of the source regions for rice, and many cultivars in this region exhibit salt tolerance comparable to the standard salt tolerant variety 'Pokkali,' such as the cultivars 'Jao Khao' and 'Luang Pratahn' (Habila et al., 2022). Time course transcriptome with weighted

Abbreviations: ABA, Abscisic acid; CDS, coding sequence; DOF, DNA-binding with one finger; LD, long day; OBF, Ocs-element binding factor; OBP, OBF binding protein; PSI, photosystem I; PSII, photosystem II; Q_A, primary acceptor plastoquinone; Q_B, secondary acceptor plastoquinone; ROS, reactive oxygen species; SD, short day; SNP, single nucleotide polymorphisms; TF, transcription factor; WT, wild-type.

* Corresponding author at: Center of Excellence in Environmental and Plant Physiology, Department of Botany, Faculty of Science, Chulalongkorn University, Bangkok, Thailand.
E-mail address: Supachitra.C@chula.ac.th (S. Chadchawan).
[1] These authors contributed equally to this work.

https://doi.org/10.1016/j.envexpbot.2024.105748
Received 6 November 2023; Received in revised form 21 March 2024; Accepted 21 March 2024
Available online 23 March 2024

co-expression network analysis of 'Luang Pratahn' seedlings predicted six gene modules that participate in salt tolerance mechanisms, including photosynthesis adaptation, root initiation, abscisic acid (ABA) response, and translational and post translational control. Among these modules, *OsOBP4* was predicted to be one of the key genes contributing to salt-tolerant phenotypes by interacting with the peptide transport 2 gene (*OsPTR2*) and *SurE* (Sonsungsan et al., 2021). However, the functions of these genes in salt tolerance mechanisms are still unclear.

Ocs-element binding factor (OBF) binding proteins (OBPs) are plant-specific transcription factors (TFs) belonging to the DNA-binding with one finger (DOF) gene family, and they contain a zinc finger DNA-binding domain (Shim et al., 2019). DOF TFs possess a bifunctional N-terminal domain that binds to the AAAG DNA core motif and mediates protein-protein interactions, and it also has a C-terminal domain that regulates the transcription factor activity (Yanagisawa and Schmidt, 1999; Xu et al., 2016; Qin et al., 2019). Of the 37 DOF TFs identified in *Arabidopsis*, 30 have been reported in rice. DOFs play key roles in developmental processes and responses to environmental cues (Hernando-Amado et al., 2012; Xu et al., 2016). OBPs are involved in gene regulation and biotic and abiotic stress responses (Lijavetzky et al., 2003). They interact with OBFs and enhance their binding to the octopine synthase gene (*ocs*), a feature of pathogen-responsive plant promoters (Zhang et al., 1995; Kang and Singh, 2000; Skirycz et al., 2006). DOF TFs have been identified and studied using phylogenetic analysis as well as expression analysis in many plant species, including rice (Gaur et al., 2011; Khan et al., 2021; Liu et al., 2021), *Arabidopsis* (Lijavetzky et al., 2003), soybean (Wang et al., 2007), foxtail millet (Zhang et al., 2017), *Brachypodium distachyon* (Hernando-Amado et al., 2012), and sorghum (Kushwaha et al., 2011); they reportedly regulate flowering and many developmental processes in plants (Huang et al., 2019). Maize DOF1 is involved in carbohydrate metabolism and nitrogen assimilation (Yanagisawa and Schmidt, 1999; Yanagisawa et al., 2004), whereas rice OsDOF24 is an important regulator of leaf senescence (Shim et al., 2019).

In *Arabidopsis*, *AtOBP* genes are involved in growth and development, particularly root growth and development. *AtOBP1* participates in the cell cycle in *Arabidopsis* roots (Skirycz et al., 2008), whereas *AtOBP2*, also called *AtDof1* (*At1g07640*), is involved in defense signaling (Skirycz et al., 2006). *AtOBP3* regulates phytochrome signaling (Ward et al., 2005) and plays an important role in plant growth and development. *AtOBP3* overexpression leads to altered root development and yellowish leaves (Kang and Singh, 2000). *AtOBP4* regulates root growth during cell elongation and differentiation but not at the cell division level (Ramirez-Parra et al., 2017) and lateral root formation in the AFB3-dependent network under the regulation of the NAC4, a TF in the nitrate response pathway (Vidal et al., 2013). Moreover, *AtOBP4* antagonistically controls *Xyloglucan endotransglucosylase 9* (*XTH9*) expression to sustain lateral root development (Xu and Cai, 2019). Although overexpression of *AtAFB3* has been shown to enhance salt stress tolerance in roots, upregulation of *AtOBP4* was not detected after 1–2 h of salt stress (Garrido-Vargas et al., 2020). In addition, *AtOBP4* regulates root hair growth by binding to *ROOT HAIR DEFECTIVE6-LIKE2* (*RSL2*) promoter (Rymen et al., 2017).

In this study, we functionally characterized the rice OsDOF8/LOC_Os02g49440 (*OsOBP4*) TF by ectopically expressing it in both wild-type (WT) *Arabidopsis* and *Atobp4* mutant (SALK_118463) and analyzed its expression patterns under drought and salinity stress. We believe that our results contribute important findings that connect stress responses in plants with food production.

2. Materials and methods

2.1. Multiple sequence alignment, motif sequence, and phylogenetic analysis of OBP4

Multiple sequence alignment was performed using the OBP4 amino acid sequences from five representatives of both monocot and dicot plants. The sequences were retrieved from the phytozome website and the Rice Genome Annotation Project database (https://phytozome.jgi.doe.gov/pz/portal.html) (http://rice.uga.edu/, 2022, August 16th), and the phylogenetic tree was constructed using CLC Genomics Workbench v12.0 (CLC Bio, Aarhus, Denmark) using the neighbor-joining method with the default parameters and a bootstrap test with 1000 replicates. The motif sequence of the OBP4 structures was identified using MEME (http://memesuite. org/meme) with the default parameters, and the maximum number of motifs was set to 10.

2.2. Plant materials and growth conditions

Arabidopsis thaliana (Col-0; CS60000) was used as the wild-type plant. All plants used in this study were in the Col-0 background. The T-DNA mutant line of *Atobp4*, i.e., SALK_118463 (At5g60850), was supplied by the Arabidopsis Biological Resource Center (Columbus, OH, USA). 'Nipponbare' rice was used for stress tolerance experiments. The seeds were surface-sterilized and placed in 9-cm round Petri plates containing 1/2 Murashige and Skoog (MS) medium with 1% (w/v) sucrose and 1% (w/v) agar. The plates were incubated for seed stratification at 4 °C in the dark for 48 h and grown in a walk-in growth chamber at 22 °C and a 16 h light/8 h dark cycle with a light intensity of 35 μmol m^{-2} s^{-1}, as previously described (Jakada et al., 2019).

2.3. Vector construction and Arabidopsis transformation

The full-length CDS of *OsOBP4* without the stop codon was amplified from the 'Pokkali' rice DNA, and the PCR product was cloned into the pENTR/D-topo vector (Invitrogen, Carlsbad, CA, USA). The *OsOBP4* coding sequence of 'Pokkali' rice has the same nucleotide sequence as 'KDML105' rice, which is the most popular rice in Thailand. However, 'Luang Pratahn' rice has a SNP prior to the stop codon, leading to a change in the last amino acid proline in 'Pokkali' and 'KDML105' rice to leucine in 'Luang Pratahn' rice (Supplementary File S1). Positive clones were recombined with the pGWB505 destination vector and confirmed using sequencing. Finally, the construct was transformed into *Agrobacterium tumefaciens* GV3101 strain and subsequently into *Arabidopsis thaliana Atobp4* mutant and wild type by floral dip transformation (Clough and Bent, 1998). Transgenic plants were selected on 1/2 MS medium supplemented with 50 μg/mL hygromycin, and T_3 homozygous lines were used for further experiments.

2.4. Transcriptional activation analysis in yeast cells

The *OsOBP4* ORF was cloned into pGBKT7 to generate pGBKT7-OsOBP4 using the primers listed in Supplementary File S2. The yeast strain AH109 was then transformed with pGBKT7, pGBKT7–53 + pGADT7-T, or pGBKT7-OsOBP4, and the transformed cells were grown on synthetic defined (SD) (-Trp) and SD (-Ade/-His/-Leu/-Trp + X-α-gal) media. The growth status and X-α-gal activity revealed the transactivation activity of OsOBP4.

2.5. Subcellular localization

To assess the subcellular localization, the 35 S::OsOBP4-GFP construct and the control 35 S::GFP empty vector were infiltrated into the epidermal layers of the onion (*Allium cepa*) bulb and incubated in the dark for 36–48 h. The GFP signal was observed under a Zeiss microscope (ZEISS Axio 10, Germany) at an excitation wavelength of 488 nm.

2.6. RNA extraction and qRT-PCR

Total RNA was isolated using the GENEzol RNA kit (Geneaid, New Taipei City, Taiwan). The cDNA library was synthesized according to the manufacturer's instructions of the cDNA Synthesis Kit for RT-PCR

(iScript, Bio-Rad, Hercules, CA, USA). The qRT-PCR was performed using the Luna qPCR SuperMix (M3003L, New England Biolabs, Ipswich, MA, USA) on a Bio-Rad CFX-96 machine system using the following reaction conditions: 94 °C for 30 s, and 40 cycles of 94 °C for 5 s, 60 °C for 15 s, and a melting curve from 65 °C to 95 °C. The fold change in gene expression in rice and *Arabidopsis* was measured using *OsEF1α* and *AtEF1α* as internal controls. Primers used are listed in Supplementary File S2. All reactions were performed in independent biological and technical triplicates.

2.7. Induction of abiotic stress

'Nipponbare' rice was used in this study for the abiotic stress experiments on rice. The 14-day-old rice seedlings were grown in solutions containing 150 mM NaCl (salinity stress), 300 mM mannitol (osmotic stress), or 10 μM ABA. Tissue samples were harvested after the required time point, frozen immediately in liquid nitrogen, and stored at −80 °C for RNA extraction.

For the germination test of *Arabidopsis* seedlings, seeds of the wild type, *Atobp4* mutant, and transgenic lines with *OsOBP4* expression in the wild-type (WT) background (*oe1*, *oe2*) and in the *Atopb4* mutant background (*rev1* and *rev2*) were surface-sterilized and germinated on 1/2 MS agar medium supplemented with 75 mM NaCl for salinity stress, 75 mM mannitol for osmotic stress, and 0.6 μM ABA for ABA stress. The germination rate was measured for 8 days after treatment.

For *Arabidopsis* phenotyping on agar, the seeds of the wild-type, *Atobp4* mutant, *oe1*, *oe2, rev1*, and *rev2* lines were surface-sterilized and germinated on 1/2 MS medium for 6 days. The seedlings were transferred to 1/2 MS medium supplemented with 75 mM NaCl to induce salinity stress conditions in square Petri dishes (120 mm × 120 mm). Seedlings transferred to medium without NaCl supplementation were used as the control. The root length, number of lateral roots, fresh weight, and dry weight were measured. Seedlings were photographed using a scanner (Epson V800 photo scanner, Japan) and analyzed using ImageJ software version 2.00-rc-43/1.50e (National Institute of Health, Bethesda, MD, USA).

The salt stress effect on flower induction was evaluated during short-day conditions (8-h light/16-h dark period) only because none of the lines showed significant differences in flowering time under long-day conditions (16-h light/8-h dark period). All *Arabidopsis* lines were germinated on 1/2 MS medium for 7 days. Then, the seedlings were transferred to soil and allowed to grow for another 7 days. Fourteen-day-old seedlings were treated with 250 mM NaCl for salinity stress, while the control plants were supplemented with filtered water of the same volume. The flowering time and number of leaves at flowering were determined. After 30 days of treatment, the plant tissues were frozen in liquid nitrogen for RNA extraction and gene expression analysis.

For the long-day experiment, chlorophyll fluorescence was determined using a Pocket PEA fluorometer (Hansatech Instrument Ltd, UK) on 0, 3, 6, 9, 12, 15, 19, and 23 days after treatment. After 27 days of treatment, the fresh weight of the *Arabidopsis* plants was measured. Then, the tissues were incubated at 60 °C for 5 days and the dry weight was determined.

2.8. Statistical analyses

The results are presented as the means ± standard error (SE) of experiments with at least three biological replicates and three technical replicates. The experiments were performed using three biological replicates and three technical replicates. One-way ANOVA was used to analyze the gene expression levels, germination rate, root length, number of lateral roots, fresh weight, dry weight, flowering time, and number of flowerings. Means were compared using Duncan's multiple range test (DMRT) at $p<0.05$ using IBM SPSS Statistics for Windows, version 29.0.1 (IBM Corp., Armonk, N.Y., USA).

3. Results

3.1. Sequence and phylogenetic analysis of OBP4

The peptide sequences (Supplementary File S3) of OsOBP4 from various crop species, namely, tomato (*Solanum lycopersicum*, Sl), potato (*Solanum tuberosum*, St), grape vine (*Vitis vinifera*, Vv), soybean (*Glycine max*, Gm), rice (*Oryza sativa*, Os), common wheat (*Triticum aestivum*, Tae), maize (*Zea mays*, Zm), cucumber (*Cucumis sativus*, Cs), and pineapple (*Ananas comosus*, Ac), were compared with that of AtOBP4 from *Arabidopsis thaliana* (*At*). The zinc finger was conserved in all the tested species (Fig. 1). SlOBP4 had the longest amino acid sequence, whereas AcOBP4 had the shortest. The highly conserved motif of the DOF gene family, an N-terminal C2-C2 zinc finger domain (50 aa, PF02701), is shown with a red box in Fig. 2A and the amino acid sequence of the C2-C2 zinc finger domain is shown in Fig. 2 B. Clustering of OBP4 sequences in maize, rice, and common wheat suggests that this gene evolved in these species after the emergence of the Poaceae family. Notably, AcOBP4 and CsOBP4 belonged to the same clade, although they were isolated from monocots and dicots, respectively (Fig. 2C).

3.2. OsOBP4 exhibits transcriptional activity and is localized in the nucleus

OBPs are among the most highly conserved TFs in plants, and they are involved in the transcriptional regulation of important genes (Hernando-Amado et al., 2012; Cao et al., 2022). Therefore, we conducted an expression assay in yeast to verify the transcriptional activation of OsOBP4 using a GAL4 reporter system. We used pGBKT7–53 + pGADT7-T as a positive control and yeast cells with empty pGBKT7 as a negative control. pGBKT7-OsOBP4 grew on SD/-Trp and SD -Trp/His/-Leu SD media and showed α-gal (α-galactosidase) activity, which indicates that OsOBP4 is a TF (Fig. 3A). In addition, we determined the subcellular location of OsOBP4 using a 35 S::OsOBP4-GFP fusion construct transiently expressed in onion (*Allium cepa*) epidermal cells. Our results showed that OsOBP4 was localized to the nucleus (Fig. 3 B).

3.3. OsOBP4 is differentially expressed in different tissues

We then assessed *OsOBP4* expression in various 'Nipponbare' rice tissues and in vegetative and flag leaves. The expression in younger leaves was higher than that in older leaves when detected in 15-day-old seedlings. During the reproductive stage (45-day-old plants), it was expressed in the flag leaves, peduncles, and spikelets (Fig. 4). These results indicate that *OsOBP4* is differentially expressed in different organs during plant development.

3.4. OsOBP4 can be induced by salt, drought, and ABA stresses

To investigate whether *OsOBP4* could be induced by abiotic stress, 15-day-old 'Nipponbare' rice seedlings were treated with nutrient solution supplemented with 150 mM NaCl, 300 mM mannitol, or 10 μM ABA. Subsequently, *OsOBP4* expression was determined in the leaf tissues collected at 0, 3, 6, 12, 24, and 48 h post treatment.

All treatments induced *OsOBP4* gene expression. After 6 h of salt stress treatment, *OsOBP4* expression was upregulated by two-fold, whereas after 24 h of salt stress, *OsOBP4* expression was upregulated by seven-fold relative to that at the beginning of the experiment, indicating the highest induction (Fig. 5A). Drought stress caused by the application of 300 mM mannitol induced greater *OsOBP4* expression than salt stress. After 3 h of drought stress, *OsOBP4* expression was approximately six-times higher than that at the beginning of the experiment. It then decreased after 12 h but was still higher than that at the starting point (0 h). The highest expression level was detected after 48 h of drought stress (Fig. 5 B). The ABA treatment induced *OsOBP4* expression after 3 h, although the level subsequently declined to normal

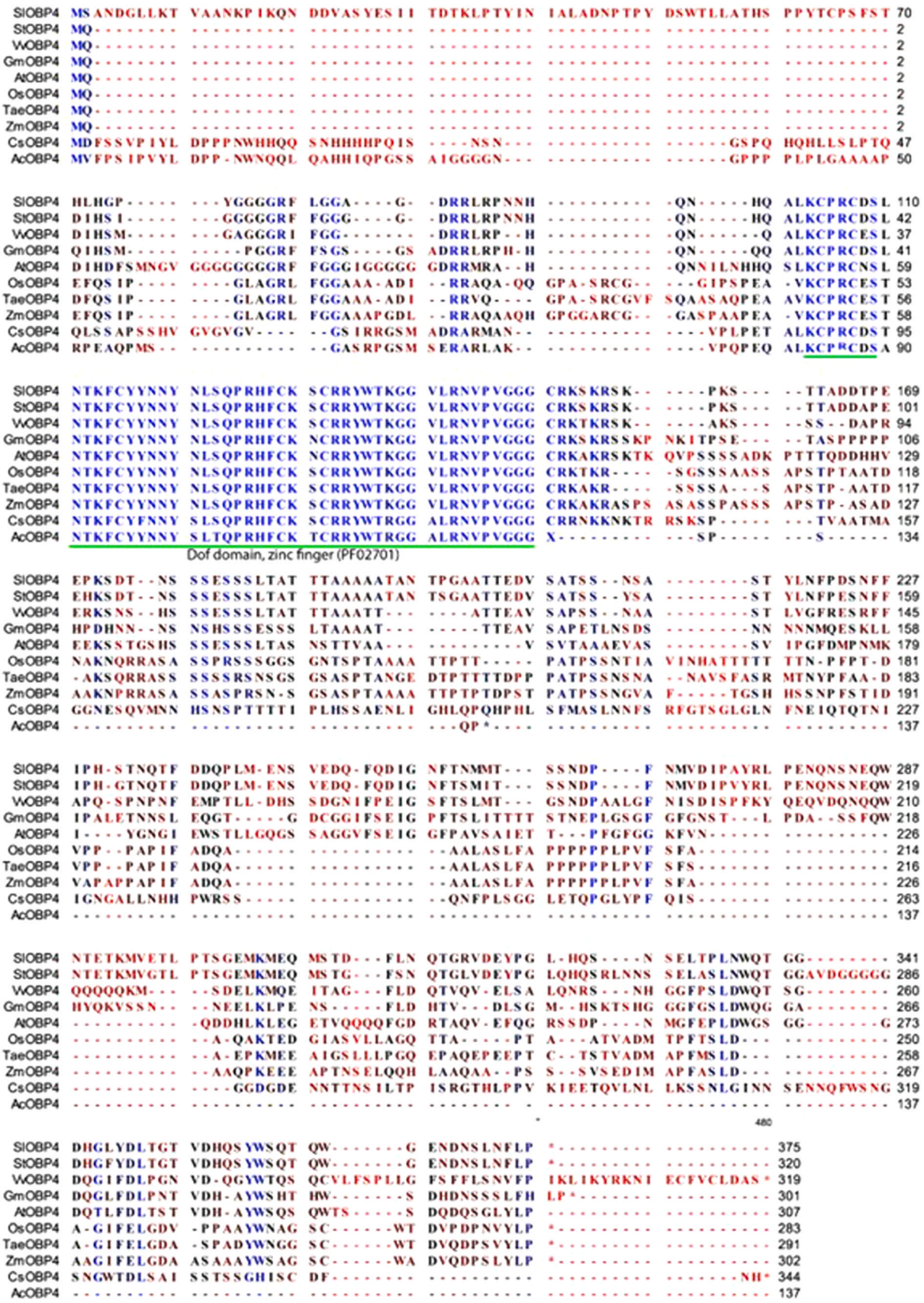

Fig. 1. Multiple sequence alignment of OsOBP4 and OBP4 from other plant species. The plant species are indicated: Sl: *Solanum lycopersicum*; St: *Solanum tuberosum*; Vv: *Vitis vinifera*; Gm: *Glycine max*; At: *Arabidopsis thaliana*; Os: *Oryza sativa*; Tae: *Triticum aestivum*; Zm: *Zea mays*; Cs: *Cucumis sativus*; and Ac: *Ananas comosus*.

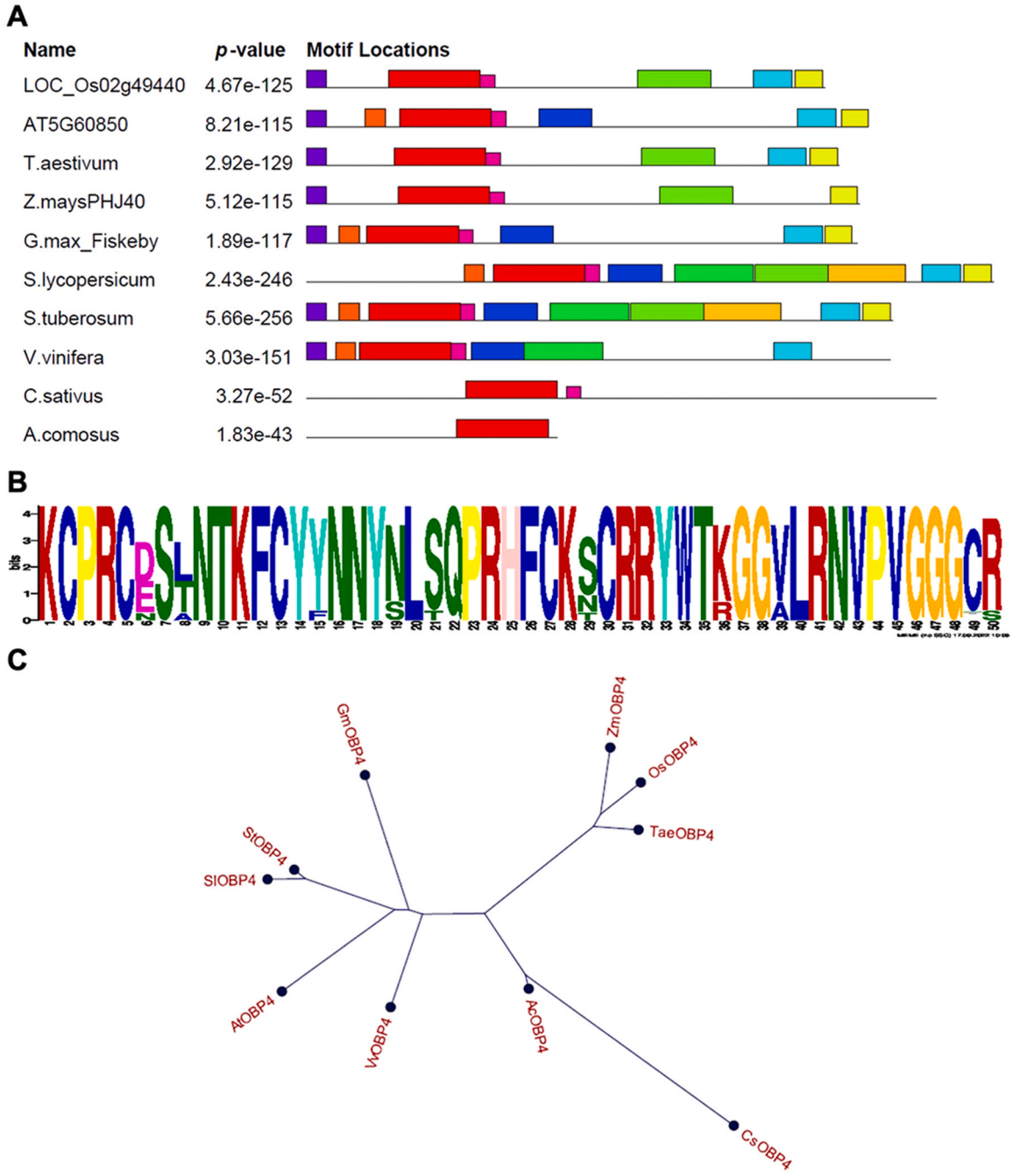

Fig. 2. Location of motifs within OBP4 from rice and other plant species (A). The plant species are indicated: Sl: *Solanum lycopersicum*; St: *Solanum tuberosum*; Vv: *Vitis vinifera*; Gm: *Glycine max*; At: *Arabidopsis thaliana*; Os: *Oryza sativa*; Tae: *Triticum aestivum*; Zm: *Zea mays*; Cs: *Cucumis sativus*; and Ac: *Ananas comosus*. The conserved motifs are demonstrated. The red box represents the C2-C2 zinc finger domain, while other colored boxes represent other conserved motifs in OBP4 protein. The sequence of C2-C2 zinc finger domain is shown in (B) and the phylogenetic analysis of this protein is demonstrated in (C). CLC genomics workbench v12 was used to align protein sequences, and a phylogenetic tree was constructed using the neighbor-joining (NJ) method, with a bootstrap value of 1000.

levels after 24 h. Although *OsOBP4* expression was enhanced after 24 and 48 h, it was lower than that observed after 3 h of treatment (Fig. 5C).

3.5. *OsOBP4 expression can complement Atobp4 mutation in root development under salt stress*

To determine whether *OsOBP4* expression can complement the *Atobp4* mutation, *OsOBP4* regulated by *35SCaMV* promoter was transformed into the *Atobp4* mutant and monitored for phenotypic changes in comparison with non-transformed *Atobp4* mutant's phenotypes under normal and salt stress conditions.

Homozygous T_3 plants were used to determine the response to salt stress during germination and seedling development. Under normal conditions, the WT germinated significantly ($p<0.05$) faster than the other lines and the *Atobp4* (*obp4*) knockout mutant had the lowest germination rate after 5 days of germination on 1/2 MS medium. After 2 days, the WT seeds showed a germination percentage of up to 98%, whereas the other lines had germination percentages of 81–90%. After 6 days, the germination percentages of all the lines were not significantly different (Fig. 6 A).

ABA inhibits *Arabidopsis* germination, and *Atobp4* mutations cause

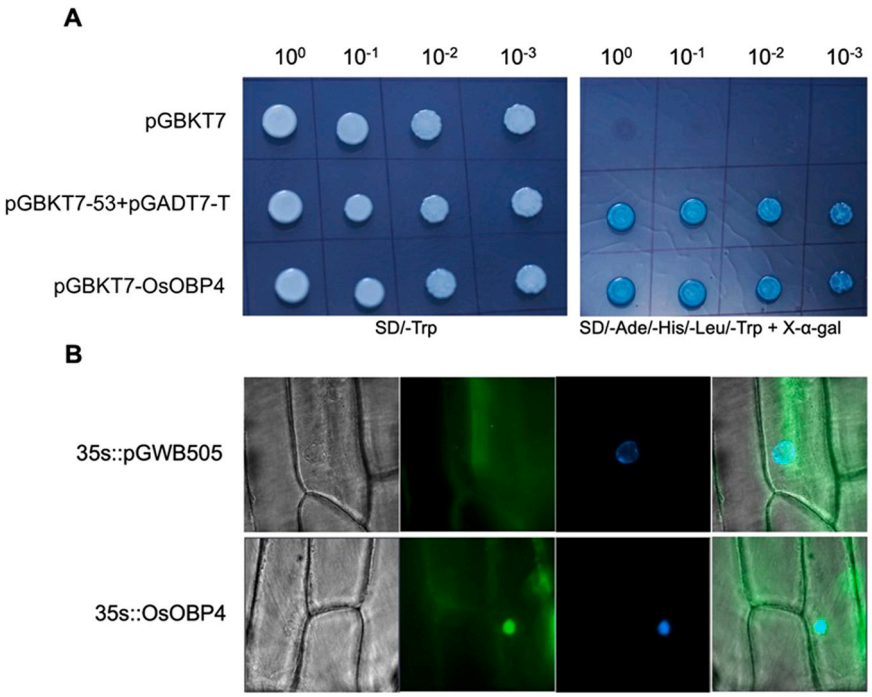

Fig. 3. Assay to assess the transcription activity of OsOBP4. Yeast cells co-transformed with pGBKT7-53 + pGADT7-T, and pGBKT7-OsOBP4. The vectors pGBKT7-53 + pGADT7-T were used as the positive control, and yeast cells with empty vector pGBKT7 were used as a negative control (A). Yeast cultures containing the respective vectors were grown on the synthetic medium supplemented with dextrose (SD) in the absence of Trp (SD/-T), and on SD medium with α-galactosidase and in the absence of Leu, Trp, His, and Ade (SD/-L -T –H –A + X-α-gal). OsOBP4-GFP localized to the nucleus. OsOBP4-GFP localization in the nucleus of onion cell (B). GFP fluorescence is represented in green and DAPI in the blue channel; scale bars = 20 μm.

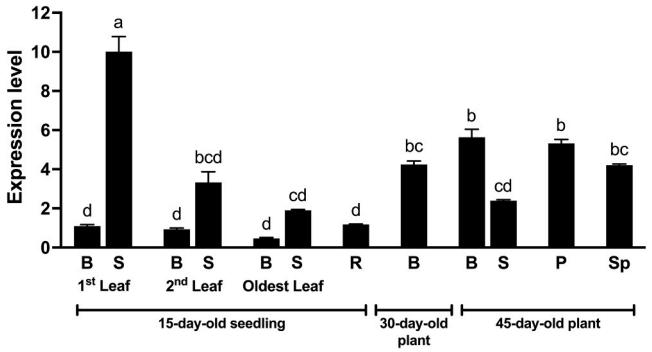

Fig. 4. Expression levels of the *OsOBP4* in different tissues at different stages of development. Gene expression is represented in change of expression against *Arabidopsis OsEF1α* calculated using the $2^{-\Delta\Delta CT}$ method (Livak and Schmittgen, 2001). Vertical bars indicate ± SE. All experiments were performed with three technical and three biological repeats. The different letters above the bars represent the significant difference among the means of expression levels analyzed by DMRT at $p<0.05$. B: leaf blade, S: leaf sheath, R: root, P: peduncle, and Sp: spikelet.

susceptibility to ABA. The *Atobp4* mutant showed a significant decrease in the germination percentage after treatment with 0.6 μM ABA. Moreover, ABA delayed germination in the WT. The maximum germination percentage was noted after 6 days of germination. The ectopic expression of *OsOBP4* in the *oe1* and *oe2* WT lines and *rev1* and *rev2* mutant lines did not change the germination percentage when compared to the background genotypes (Fig. 6 B).

Salt and osmotic stress caused a decrease in germination rates. After 8 days of germination, only 82% and 68% of the WT and *Atobp4* mutant seeds germinated, respectively. The ectopic expression of *OsOBP4* in the mutant lines *rev1* and *rev2* caused a decrease in germination percentage to 49% and 33%, respectively. Only *oe1* line showed a germination percentage similar to that of the WT, whereas the *oe2* germination percentage decreased (Fig. 6 C). Notably, no significant difference occurred in the germination rate among these lines under osmotic stress; however, delayed germination was detected in all lines (Fig. 6 D).

To investigate the effect of *Atobp4* mutation at seedling stage, the 7-day-old seedlings were transferred to the 1/2 MS medium supplemented with 100 mM NaCl for 7 days and compared with the normally grown seedlings as a control. Under normal conditions, the *Atobp4* mutant had shorter roots than the WT, whereas the ectopic expression of *OsOBP4* enhanced root development by increasing the root length. The fresh and dry weights of *oe1* and *oe2* were similar to those of the WT, whereas those of *rev1* were similar to those of *Atobp4* (Supplementary Fig. S1).

Phenotyping of ectopic expression lines under salinity stress showed that both *oe1* and *oe2* exhibited similar root lengths as the WT. However, the *rev1* and *rev2* lines had significantly ($p<0.05$) longer roots than the *Atobp4* mutant lines after 6 days of exposure to salt stress (Fig. 7A).

Additionally, the *rev1* and *rev2* lines showed a significantly higher number of lateral roots on day 6 after treatment compared to that of both the WT and *obp4* mutant lines (Fig. 7B). No significant difference was noted in fresh weight and dry weight among the lines after 12 days under salinity, although the dry weight of the ectopically expressed *OsOBP4* was higher than that of the WT and *Atobp4* mutants (Fig. 7C and Fig. 7D). The phenotypes of the ectopic expression lines under normal conditions and salinity stress 12 days after treatment are shown in Fig. 7E and Fig. 7F, respectively.

To investigate the role of OBP4 during a later plant developmental stage, STRING analysis was performed to predict the possible interaction between OBP4 protein and others. OsOBP4 was shown to connect with proteins related to flowering regulation (OsMADS14), photosynthesis process, especially with light reaction (OsJ_23098 (photosystem I protein-like protein) and OsTHF1 (thylakoid formation 1)), expansin (EXPA7) and aquaporin (TIP4 – 1) (Fig. 8). Therefore, flowering time under normal and salt stress conditions was monitored.

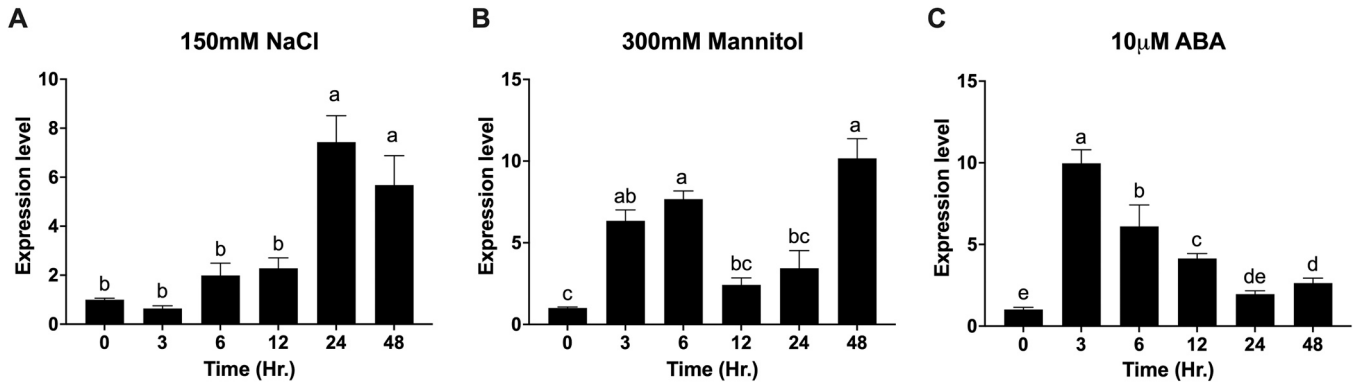

Fig. 5. Expression levels of *OsOBP4* in response to abiotic stress induction, salt stress (150 mM NaCl) (A), drought stress (300 mM mannitol) (B), and 10 μM ABA (C). Expression of *OsOBP4* was measured at different time points (0, 3, 6, 12, 24, and 48 h after treatment). Gene expression is represented against *OsEF1α* calculated using the $2^{-\Delta\Delta CT}$ method. Vertical bars indicate ± SE, and asterisks indicate significantly different values than the control treatment (0 h) (*** $p < 0.001$). All experiments were performed with three technical and three biological replications.

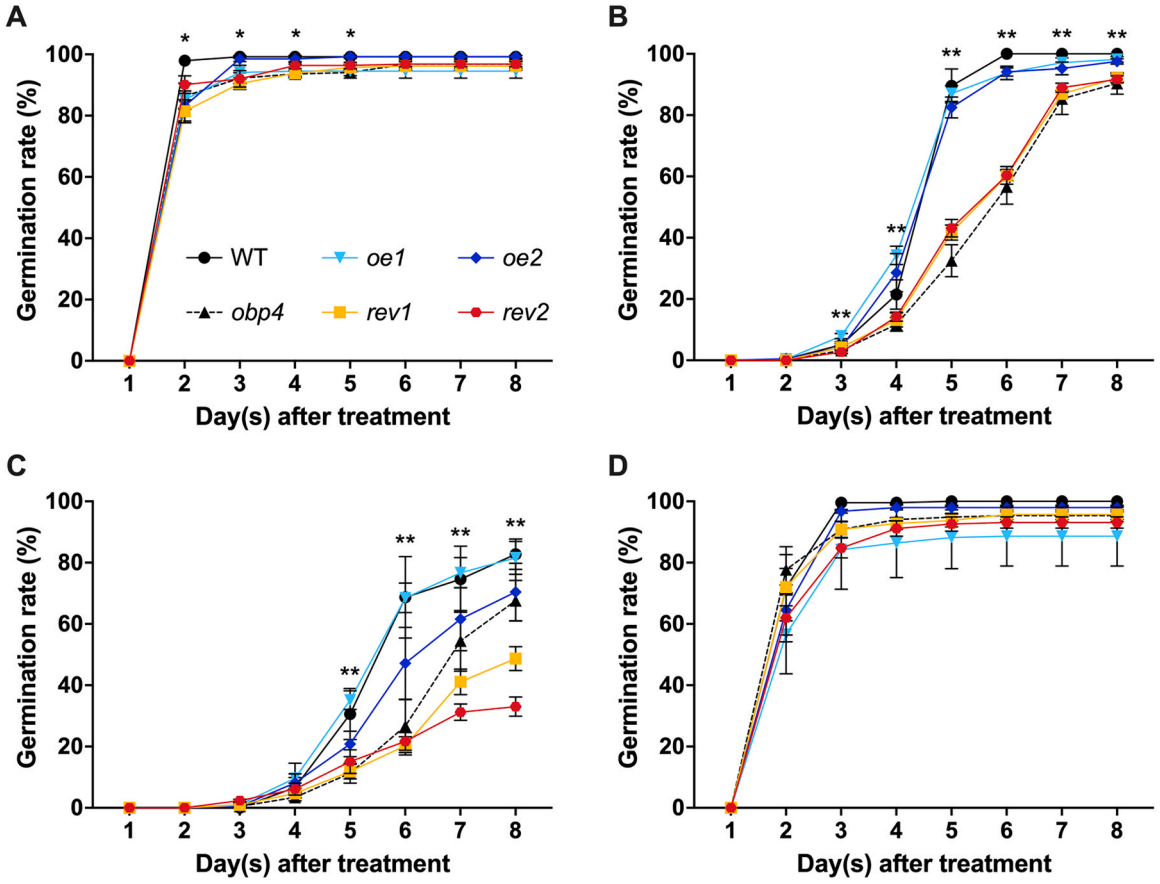

Fig. 6. Germination rate of the WT, *obp4*, *oe1*, *oe2*, *rev1*, and *rev2* lines under normal conditions (A), 0.6 μM ABA (B), 75 mM NaCl (C), and 75 mM mannitol (D). Statistical significance set to *$p < 0.05$ and ** $p < 0.01$. The experiments were performed with four replicates.

3.6. OsOBP4 expression showed an interaction with flowering regulation genes under salt stress under short-day (SD) conditions

The different flowering responses were revealed under the short-day (SD) conditions only. Under the long-day (LD) conditions, similar flowering times were detected in all lines. For normal-growth conditions under SD, only 60% of both the WT and *obp4* mutant lines flowered at 43–47 days after germination (DAG) (Table 1 and Fig. 9 A), whereas all *oe1* and *rev2* plants (100%) flowered. However, the transgenic lines *oe2* and *rev1* showed a lower flowering percentage than *oe1* and *rev2*, respectively. Salt stress increased the flowering percentage of all lines, except *obp4* mutant and *rev1*. Lines *oe1* and *rev2* (100%) showed similar flowering to that under normal growth condition (Table 1).

The flowering time and number of rosette leaves of each line was investigated as shown in Fig. 9. In the control condition (no stress), the transgenic lines with *OsOBP4* expression, *oe1*, *rev1* and *rev2*, showed a decrease in flowering time (Fig. 9 A). The number of rosette leaves at flowering of the transgenic lines with *OsOBP4* expression was significantly lower than that of the background genotype (Fig. 9B). Line *oe2* was the only transgenic line that showed no significant changes

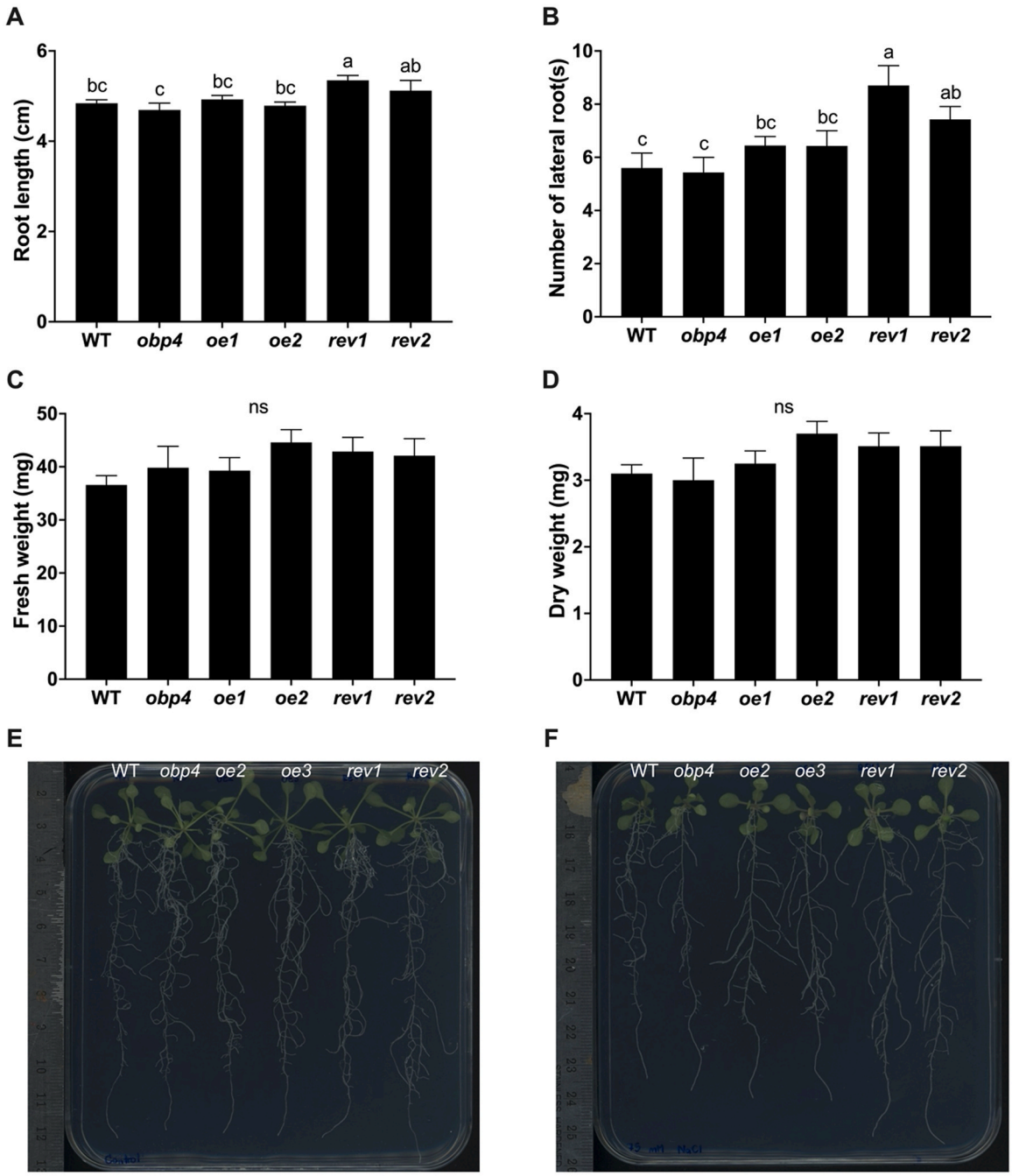

Fig. 7. Phenotype of the WT, *obp4*, *oe2*, *oe3*, *rev1,* and *rev2* lines, including the root length, under 75 mM NaCl at 6 DAT (A), number of lateral roots under 75 mM NaCl at 6 DAT (B), fresh weight per plant under 75 mM NaCl at 12 DAT (C), dry weight per plant under 75 mM NaCl at 12 DAT (D), morphology of plants under normal conditions at 12 DAT (E), and morphology of plants under 75 mM NaCl at 12 DAT (F). All experiments were performed with five replicates. Letters above the bars represent the significant difference among means ($p < 0.05$). Error bars show the standard error of five replicates.

($p<0.05$) in flowering time and number of leaves at flowering. Salt stress caused a significantly ($p<0.05$) shorter flowering time (Fig. 9 A) and lower number of rosette leaves at flowering in the *obp4* mutant but not in the other lines (Fig. 9 B). These findings support the role of OBP4 in flowering regulation during salt stress condition.

To confirm the interaction between the OBP4 protein and MADS protein in flowering regulation, as predicted by STRING, the expression of OsMAD14 orthologs in Arabidopsis, AT1G69120 (AGL7, AP1) and AT1G26310 (AGL10, CAL) (Fig. 8), were measured at the end of the experiment (51 DAG) (Fig. 10). The transgenic lines with *OsOBP4* expression, *oe1* and *rev2*, were used as representatives for *AGL7* and *AGL10* expression in comparison with the WT and *obp4* mutant.

Under normal conditions, *AGL7* expression in the *opb4* mutant was significantly higher than that in the WT and revertant line *rev2* (Fig. 10 A). *AGL10* expression also showed similar increase (Fig. 10 B). Salt stress induced the expression of both *AGL7* and *AGL10* in the WT but significantly inhibited *AGL7* expression in the *obp4* mutant. In the *oe1* line, salt stress induced both *AGL7* and *AGL10* expression. In *rev2*, slight induction of *AGL7,* but not *AGL10,* was detected (Fig. 10 A). These findings suggested that under salt stress, a lack of *OBP4* expression affected *AGL7* expression but not *AGL10* expression. The expression of *OsOBP4* in the WT could enhance *AGL7* and *AGL10* expression under salt stress, as shown in *oe1*.

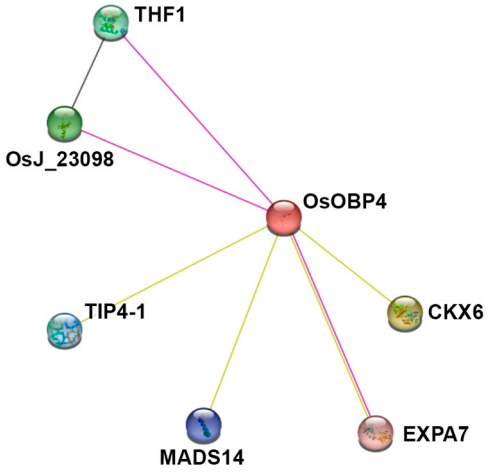

Fig. 8. Interaction of OsOBP4 with other proteins based on the STRING database.

Table 1
Flowering (%) when the WT, *obp4* mutant, *oe1*, *oe2*, *rev1*, and *rev2 Arabidopsis* lines were grown under short-day (SD) conditions with normal or salt stress.

line	% Flowering	
	Normal	Salt stress
WT	60	80
obp4	60	40
oe1	100	100
oe2	50	60
rev1	80	60
rev2	100	100

3.7. OBP4 is involved in energy dissipation in photosynthesis under salt stress condition

Since an interaction was predicted between OsOBP4 and proteins related to the thylakoid membrane, OsTHF1 and OsJ_23098, that encodes photosystem I protein-like proteins, chlorophyll fluorescence during salt stress was investigated to distinguish the response among the WT, *Atobp4* mutant, *oe1*, *oe2*, *rev1*, and *rev2* lines. After the salt stress treatment, photosynthesis parameters were determined via JIP-test analysis (Li et al., 2017) on days 0, 3, 6, 9, 12, 15, 19, and 23 after treatment. The chlorophyll induction curves or OJIP curves of all lines were similar at 0–19 days after treatment. At 23 days after the treatment, differences in the OJIP curves were detected under salt stress conditions (Fig. 11).

The chlorophyll induction curve of all the plant lines was similar under normal conditions (Fig. 11 A). However, when exposed to salinity stress, the *Atobp4* mutant line showed the lowest fluorescence intensity while *rev2* showed the highest fluorescence intensity (Fig. 11 B). This suggested that the photosystem of the *Atobp4* mutant was more sensitive to salt stress than WT. The expression of *OsOBP4* in *rev1* and *rev2* could stabilize the chlorophyll fluorescence levels under salt stress conditions (Fig. 11 A and B), suggesting the role of *OsOBP4* in photosystem maintenance under salt stress. This finding supported the interaction of OsOBP4 with proteins functioning in the thylakoid membrane (Fig. 8).

The photosynthetic parameters of the *Atobp4*, *oe1*, and *rev1* lines had higher performance index of light absorption (PI_{ABS}) and total performance index (PI_{total}) values under normal conditions (Fig. 11 C). However, under salinity stress, only the *Atobp4* mutant line showed a different pattern of photosynthetic parameters compared with the other lines and displayed lower φEo, φRo, ψEo, δRo, PI_{ABS}, and PI_{total} but higher ABS/RC, TRo/RC, and DIo/RC (Fig. 11 D).

The parameters in the figure are described below (Li et al., 2017):

φPoMaximum quantum yield for primary photochemistry

φEoQuantum yield of the electron transport flux from Q_A to Q_B

φRoQuantum yield for reduction of end electron acceptors at the PSI acceptor side

ψEoEfficiency/probability with which a PSII trapped electron is transferred from Q_A to Q_B

δRoEfficiency/probability with which an electron from Q_B is transferred until PSI acceptor

ABS/RCAbsorbed photon flux per RC

TRo/RCTrapping

ETo/RCElectron transport flux per RC

REo/RCElectron flux reducing end electron acceptors at the PSI acceptor side per RC

DIo/RCDissipation as heat and fluorescence per RC

PI_{ABS}Performance index on the absorption basis

PI_{total}Total performance index up to the PSI end electron acceptors

3.8. Atobp4 mutant became more susceptible to salt stress determined using plant growth and OsOBP4 expression reversed this effect

To investigate the response of plant growth under salt stress, all lines were grown in soil for 14 days under LD conditions. Then, salt stress was induced by the addition of 300 mM NaCl solution, whereas the control plants were maintained with filtered water at the same volume daily.

Salinity stress had a negative effect on the fresh and dry weights of the vegetative parts of all lines. The *Atobp4* mutant line had the highest reduction in both fresh weight and dry weight, suggesting the importance of *AtOBP4* in salt tolerance. *OsOBP4* expression in *Atobp4* mutant

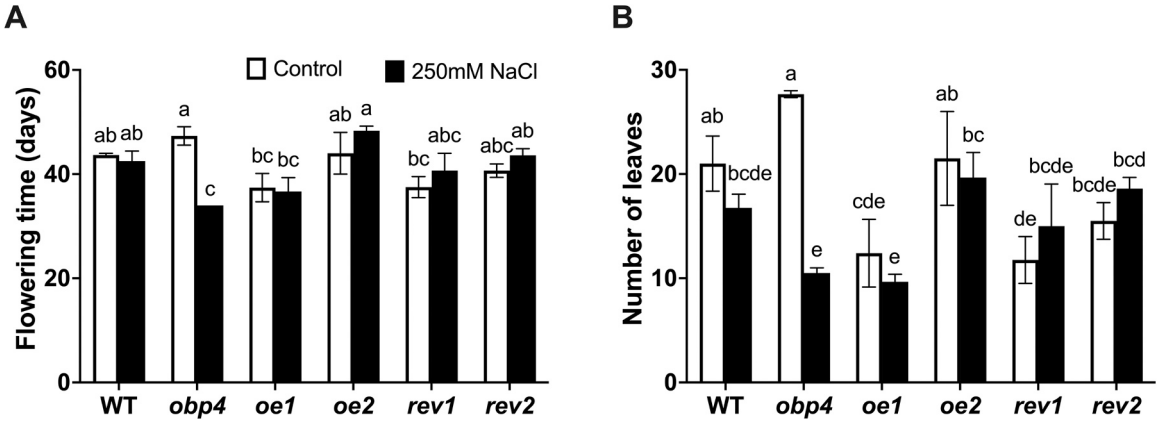

Fig. 9. Flowering time (A) and number of leaves at the flowering stage (B) of the WT, *obp4* mutant, *oe1*, *oe2*, *rev1*, and *rev2* under short-day (8/16 light/dark) condition. Letters above the bars represent significant difference among means ($p < 0.05$). Error bars show standard error of at least three replicates.

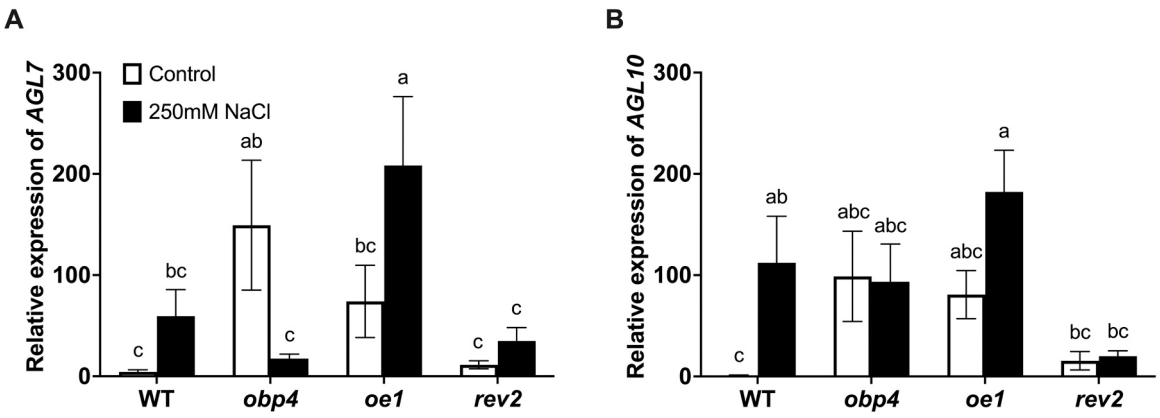

Fig. 10. Relative expression of the *AGL7* gene (A) and *AGL10* gene (B) in the WT, *obp4*, *oe1*, and *rev2* lines under normal and salinity stress (250 mM NaCl). Letters above the bars represent significant difference among means ($p < 0.05$). Error bars show the standard error of at least three replicates.

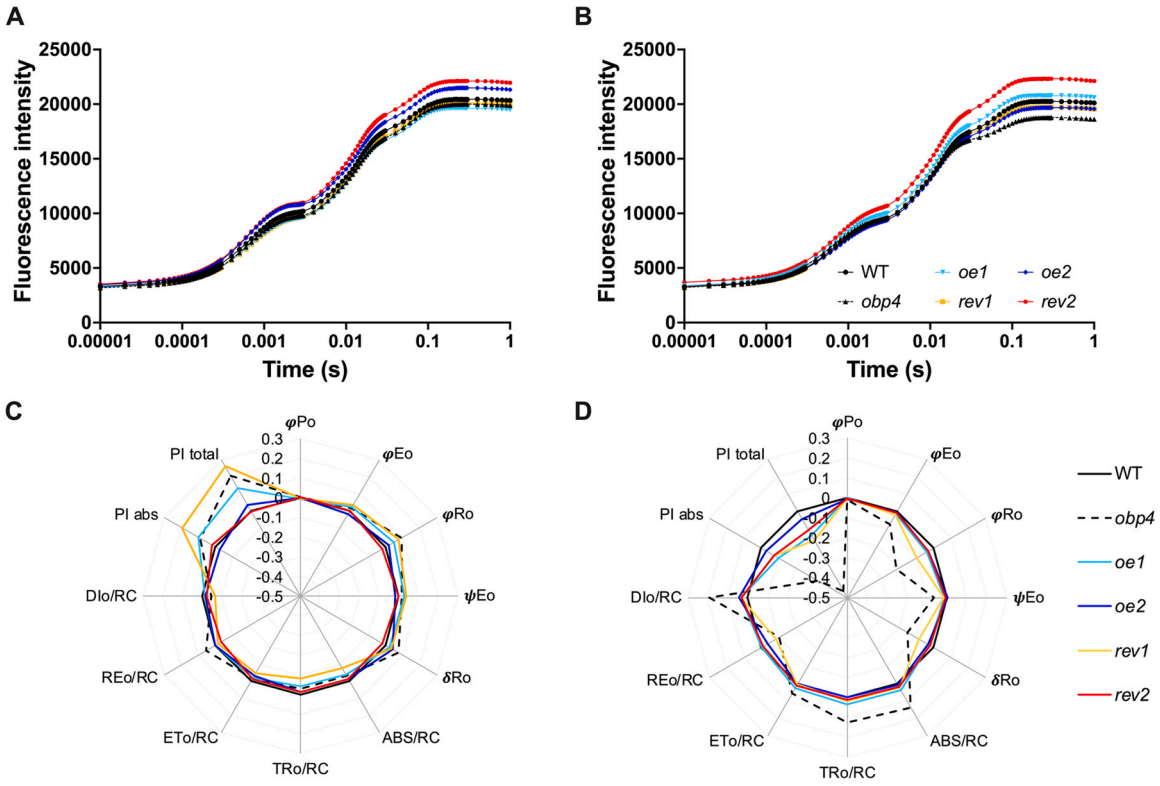

Fig. 11. OJIP parameters of the WT, *obp4*, *oe1*, *oe2*, *rev1*, and *rev2 lines:* chlorophyll induction curve under normal conditions (A), chlorophyll induction curve under salinity stress (B), spider chart of photosynthetic parameters under normal conditions (C), and spider chart of photosynthetic parameters under salinity stress (D). All experiments were performed with four biological replications.

background could reverse this effect by decreasing the fresh weight and dry weight reduction percentages to a level similar to that of the WT. However, ectopic expression of *OsOBP4* did not enhance salt tolerance in the WT background, as shown in the *oe1* and *oe2* lines (Fig. 12). Additionally, to investigate the effect on the reproductive growth, the number of inflorescences per plant was evaluated. Salt stress caused a reduction in inflorescence number per plant in all lines, except for the *rev1* line (Fig. 13 A). In the WT background, the percent reduction in inflorescence number was increased. However, in the *Atobp4* mutant background, *OsOBP4* expression in the *rev1* and *rev2* lines could minimize the percent reduction in inflorescence number (Fig. 13 B). Moreover, the fresh weight per inflorescence was similar for all lines (data not shown). These findings suggest that *OBP4* is involved in supporting plant reproduction under salt stress and LD conditions.

4. Discussion

Abiotic stress activates multiple stress-response signaling cascades in plant cells. TFs that regulate the expression of downstream stress-related genes enable plants to adapt to harsh environmental conditions. Therefore, identifying and characterizing genes associated with abiotic stress responses and flowering in rice is important for improving production. However, to the best of our knowledge, the functional characterization of DOFs remains limited, with only 5 out of the 30 predicted DOFs characterized in detail (Washio, 2003; Yamamoto et al., 2006; Iwamoto et al., 2009; Li et al., 2009; Santos et al., 2012).

DOFs are plant-specific TFs (Riechmann et al., 2000; Yanagisawa, 2004). OBPs are a class of DOFs that play an essential role in the stress response and flowering in rice (Riechmann et al., 2000; Ma et al., 2015;

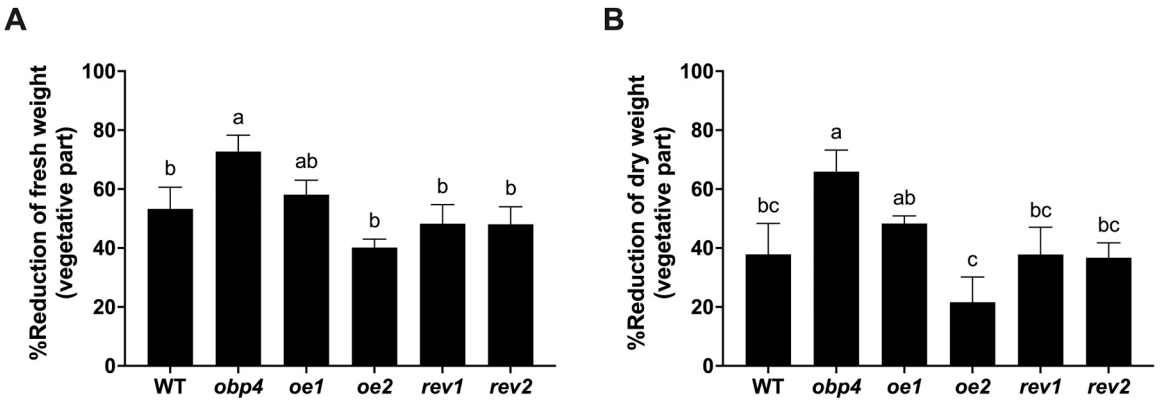

Fig. 12. Growth parameters of the vegetative parts of the WT, *obp4*, *oe1*, *oe2*, *rev1*, and *rev2* lines, as indicated by the percent reduction of fresh weight (A) and dry weight (B) under salinity stress compared to normal conditions. Letters above the bars represent the significant difference among means ($p < 0.05$). Error bars show the standard error of four replicates.

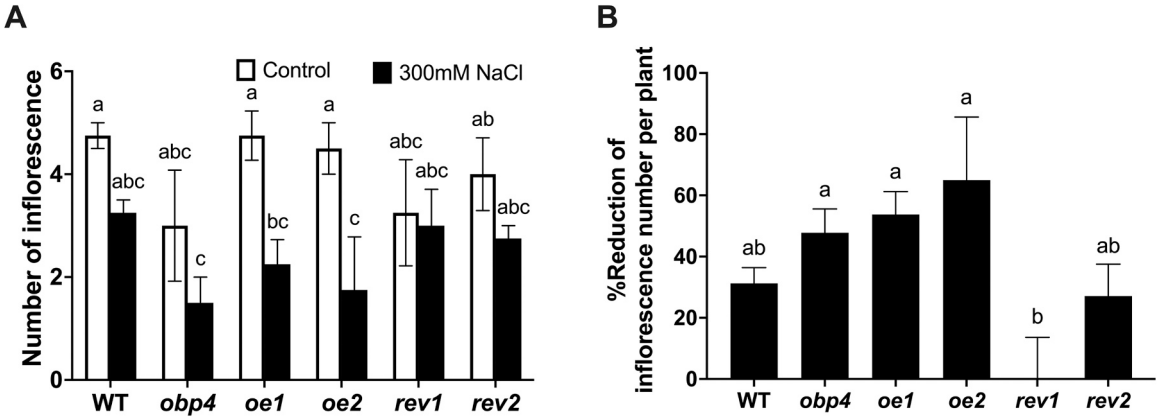

Fig. 13. Growth parameters of the reproductive parts of the WT, *obp4*, *oe1*, *oe2*, *rev1* and *rev2* lines, as shown by the number of inflorescences (A) and percent reduction of inflorescence number per plant. Letters above the bars represent significant difference among means ($p < 0.05$). Error bars show the standard error of four replicates.

Ramirez-Parra et al., 2017; Qin et al., 2019). Systematic classification based on sequence alignment, phylogenetics, and gene structure is essential for functional analysis of OBP4 in different plant species. *In silico* analysis revealed the existence of a C2-C2 zinc finger domain in this protein (Fig. 1). This domain is highly conserved and a characteristic signature of DOFs in plants (Kushwaha et al., 2011). The C2-C2 domain is important for the regulation and interaction of many genes, particularly during stress and flowering (Qin et al., 2019). The functional identity of OBPs is determined by their unique signaling domain of 50 amino acids (PF02701). Many studies have suggested that motif distribution and gene structure can be used as supporting evidence for evolutionary relationships between the genes of different plant species (Gaur et al., 2011; Cao et al., 2022). The rice OBP4 protein was incorporated with OBP4 proteins from other species to construct a phylogenetic tree, and OsOBP4 was classified into the same clade as OBP4 from three monocot crop plants: rice, maize, and wheat (Fig. 2 C). A phylogenetic tree is important for functional characterization (Hernando-Amado et al., 2012). Phylogenetic trees have also been used to demonstrate the evolutionary conservation of plants (Kushwaha et al., 2011). Many studies classified OBP4 among the DOFs that have important functions in plant growth and development (Kushwaha et al., 2011; Le Hir and Bellini, 2013; Khan et al., 2021). Similar to other OBPs and DOF proteins, OsOBP4 contains a DOF domain and can activate transcription in yeast (Fig. 3 A). Additionally, we found OsOBP4-GFP in onion epidermis localized to the nuclei (Fig. 3 B). The composition and structure of the motifs of DOFs and many TFs are related to their DNA-binding ability, protein-protein interactions, and transcriptional activity (Khan et al., 2021; Cao et al., 2022). The DOF also determines the localization and biological functions of OBP genes (Li et al., 2009, 2016; Cao et al., 2022). Consistent with previous studies, OBP4 showed highly conserved motifs, protein and gene sequences, and phylogenetic relationships among plants.

Several studies have suggested that plant OBPs regulate developmental and adaptive responses to environmental stress (Ramirez-Parra et al., 2017; Qin et al., 2019; Shim et al., 2019). *OsOBP4* showed differential expression in different tissues of rice (Fig. 4), and the qPCR data revealed that *OsOBP4* was induced when *Oryza sativa* was treated with 150 mM NaCl, 300 mM mannitol, or 10 μM ABA (Fig. 5). These findings are consistent with abiotic stress-related induction of *OBP* expression in other species (Li et al., 2016; Liu et al., 2019).

Previous research has suggested that OBP4 regulates cell growth in *Arabidopsis* and represses genes involved in root hair development, water transport, and stress responses (Xu et al., 2016; Rymen et al., 2017; Xu and Cai, 2019). Ectopic *OsOBP4* expression, especially in *rev1* and *rev2*, revealed that the protein affects root developmental response under salt stress, which is consistent with the function of *OBP* genes in other species.

According to the STRING database, OsMADS14 was predicted to be related to OsOBP4 (Fig. 8). The orthologous genes of OsMADS14 in *Arabidopsis,* AGL7 (AT1G69120), and AGL10 (AT1G26310), are reportedly involved in flowering regulation (Smyth, 2023; Lai et al., 2021). The mutation in *AtOBP4* caused flowering inhibition under salt

stress and SD conditions (Table 1). The expression of *OsOBP4* in *rev1* and *rev1* could rescue this phenotype. However, the flowering time and number of leaves at flowering in the *Atobp4* mutant were significantly lower than those of the WT, suggesting the role of *AtOBP4* in flower regulation. The *OBP* genes are important regulators of pathways controlling flowering and responses to environmental stress (Kang and Singh, 2000; Le Hir and Bellini, 2013). By regulating the expression of MADS-BOX TRANSCRIPTION FACTOR 14 (MADS14), FLOWERING LOCUS C (FLC), FLOWERING LOCUS T (FT), and SUPPRESSOR OF OVEREXPRESSION OF CONSTANS 1 (SOC1), many DOFs regulate abiotic and biotic stress-related genes and the flowering pathway (Wu et al., 2015). In addition, DOF proteins are important regulators of flowering under long-day and short-day photoperiods in rice (Huang et al., 2019). Similarly, OBP4 was found to regulate phytochrome and cryptochrome signaling in *Arabidopsis* leading to the regulation of flowering time (Ward et al., 2005). Our results support the fact that the function of the *OBP4* gene can regulate the expression level of *AGL7* (Fig. 10), which may result in recovery flowering time and number of leaves when plants are exposed to salinity stress to be similar to WT (Table 1). This suggests that OBP4 acts upstream of AGL7, which regulates the action of SOC1 and AGL24 for floral meristem initiation (review: Li et al., 2024). Moreover, this function was found only for the SD condition, suggesting that OsOBP4 may function in flowering regulation *via* the photoperiod scheme.

Two proteins that function in the chloroplast, namely, OsJ_23098, which encodes photosystem I protein-like protein, and OsTHF1, which encodes thylakoid formation I, were predicted to interact with OsOBP4 (Fig. 8). Therefore, chlorophyll fluorescence and related parameters were measured for the response during salt stress. Interestingly, the *Atobp4* mutant showed a decrease in performance index (PI_{ABS} and PI_{total}) while the revertants by *OsOBP4* (*rev1* and *rev2*) showed a similar response as the WT (Fig. 11 D). Moreover, the *Atobp4* mutant showed increased the absorption of photon flux (ABS/RC) and trapping excitation flux (TRo/RC) but high energy dissipation as heat and fluorescence (DIo/RC). These changes could cause a low level of PI_{ABS} and PI_{total} as the energy could not be used for photochemical reaction efficiently. When we focused on the flux ratio of PSII and PSI, the *Atobp4* mutant showed a loss of efficiency because PSII trapped and transferred energy to Q_A and Q_B (ψEo), efficiency with which an electron from Q_B is transferred until PSI acceptor (δRo), quantum yield of the electron transport flux from Q_A to Q_B (φEo), and quantum yield for reduction of end electron acceptors at the PSI acceptor side (φRo) were lowered than WT and other transgenic lines. These results reveal that the *Atobp4* mutant can cause a low performance index of light reaction (Fig. 11) and a high reduction of fresh weight and dry weight (Fig. 12). The ectopic expression of *OsOBP4* can recover these functions so that the values resemble those of the WT. The ability of *rev1* and *rev2* to maintain the efficiency of the photosystem may lead to lower reductions in both vegetative and reproductive tissues under salt stress (Figs. 12 and 13). However, OsOBP4 did not show positive effects on germination under salt stress conditions (Fig. 6 C). This suggests that OsOBP4 protein could not substitute for the function of AtOBP4 in the germination stage. However, it could partially substitute for the salt-tolerant functions of AtOBP4 in later developmental stages.

5. Conclusion

Collectively, we demonstrated that *OsOBP4* plays an important role in regulating environmental stress and flowering time under SD conditions. Overexpression of *OsOBP4* led to the enhancement of salt tolerance by enhancing root growth, *AGL7* expression for floral meristem induction, and light reaction process maintenance in the chloroplast. These findings could provide a better understanding of the regulation of environmental stress in rice.

Funding

This research was supported by the Thailand Science Research and Innovation Fund Chulalongkorn University (CU_FRB65_food (5)_113_23_43) and the Network Strengthening Fund Program 16 (B16F640103). BHJ received a C2F postdoctoral scholarship. CP was supported by the Ratchadapisek Somphot Fund for Postdoctoral Fellowships at Chulalongkorn University. TBS was supported by an RGJ-Asean scholarship. AS was supported by the Asean-Non-Asean Scholarships, Chulalongkorn University.

Author statement

SC, CP, and BHJ conceived and designed the study. BHJ, CP, AS, TB and TBS collected data, and analyzed and interpreted the results. BHJ, CP, and SC drafted the manuscript. SC and CP revised the manuscript. All the authors reviewed the results and approved the final version of the manuscript.

CRediT authorship contribution statement

Supachitra Chadchawan: Writing – review & editing, Supervision, Project administration, Methodology, Funding acquisition, Formal analysis, Conceptualization. **Triono Bagus Saputro:** Investigation. **Teerapong Buaboocha:** Writing – review & editing, Investigation, Conceptualization. **Bello Hassan Jakada:** Writing – original draft, Methodology, Investigation, Conceptualization. **Chutarat Punchkhon:** Writing – review & editing, Writing – original draft, Visualization, Validation, Methodology, Investigation, Formal analysis. **Achmad Syarifudin:** Investigation.

Declaration of Competing Interest

The authors declare that they have no known competing financial interests or personal relationships that could have appeared to influence the work reported in this paper

Appendix A. Supporting information

Supplementary data associated with this article can be found in the online version at doi:10.1016/j.envexpbot.2024.105748.

References

Aslam, M., Sugita, K., Qin, Y., Rahman, A., 2020. Aux/IAA14 regulates microRNA-mediated cold stress response in *Arabidopsis* roots. Int. J. Mol. Sci. 21 https://doi.org/10.3390/ijms21228441.

Aslam, M., Fakher, B., Greaves, J.G., Jakada, B.H., Qin, R., Qin, Y., 2022. A CBL-interacting protein kinase, AcCIPK18, from *Ananas comosus* regulates tolerance to salt, drought, heat stress and Sclerotinia sclerotiorum infection in *Arabidopsis*. Environ. Exp. Bot. 194, 104728 https://doi.org/10.1016/j.envexpbot.2021.104728.

Bailey-Serres, J., Parker, J.E., Ainsworth, E.A., Oldroyd, G.E.D., Schroeder, J.I., 2019. Genetic strategies for improving crop yields. Nature 575, 109–118. https://doi.org/10.1038/s41586-019-1679-0.

Bhatt, T., Sharma, A., Puri, S., Minhas, A.P., 2020. Salt tolerance mechanisms and approaches: future scope of halotolerant genes and rice landraces. Rice Sci. 27, 368–383. https://doi.org/10.1016/j.rsci.2020.03.002.

Cao, X., Wan, W., Mao, H., Yin, D., Deng, X., Yan, H., Ren, L., 2022. Genome-wide identification and expression analysis of dof transcription factors in lotus (*Nelumbo nucifera* Gaertn.). Plants 11. https://doi.org/10.3390/plants11152057.

Clough, S.J., Bent, A.F., 1998. Floral dip: a simplified method for Agrobacterium-mediated transformation of *Arabidopsis thaliana*. Plant J. 16, 735–743. https://doi.org/10.1046/j.1365-313x.1998.00343.x.

Garrido-Vargas, F., Godoy, T., Tejos, R., O'Brien, J.A., 2020. Overexpression of the auxin receptor *AFB3* in *Arabidopsis* results in salt stress resistance and the modulation of NAC4 and SZF1. Int. J. Mol. Sci. 21, 9528. https://doi.org/10.3390/ijms21249528.

Gaur, V.S., Singh, U.S., Kumar, A., 2011. Transcriptional profiling and in silico analysis of dof transcription factor gene family for understanding their regulation during seed development of rice *Oryza sativa* L. Mol. Biol. Rep. 38, 2827–2848. https://doi.org/10.1007/s11033-010-0429-z.

Habila, S., Khunpolwattana, N., Chantarachot, T., Buaboocha, T., Comai, L., Chadchawan, S., Pongpanich, M., 2022. Salt stress responses and SNP-based phylogenetic analysis of Thai rice cultivars. Plant Genome 15, e20189.
Hernando-Amado, S., González-Calle, V., Carbonero, P., Barrero-Sicilia, C., 2012. The family of dof transcription factors in *Brachypodium distachyon*: phylogenetic comparison with rice and barley DOFs and expression profiling. BMC Plant Biol. 12, 202. https://doi.org/10.1186/1471-2229-12-202.
Huang, Y., Han, Z., Cheng, N., Luo, M., Bai, X., Xing, Y., 2019. Minor effects of 11 dof family genes contribute to the missing heritability of heading date in rice (*Oryza sativa* L.). Front. Plant Sci. 10, 1739. https://doi.org/10.3389/fpls.2019.01739.
Iwamoto, M., Higo, K., Takano, M., 2009. Circadian clock- and phytochrome-regulated dof-like gene, Rdd1, is associated with grain size in rice. Plant Cell Environ. 32, 592–603. https://doi.org/10.1111/j.1365-3040.2009.01954.x.
Jakada, B.H., Aslam, M., Fakher, B., Greaves, J.G., Li, Z., Li, W., Lai, L., Ayoade, O.A., Cheng, Y., Cao, S., Li, G., Hu, J.M., Qin, Y., 2019. Identification of SWI2/SNF2-related 1 chromatin remodeling complex (SWR1-C) subunits in pineapple and the role of pineapple SWR1 COMPLEX 6 (AcSWC6) in biotic and abiotic stress response. Biomolecules 9. https://doi.org/10.3390/biom9080364.
Kang, H.G., Singh, K.B., 2000. Characterization of salicylic acid-responsive, *Arabidopsis* Dof domain proteins: overexpression of OBP3 leads to growth defects. Plant J. 21, 329–339. https://doi.org/10.1046/j.1365-313x.2000.00678.x.
Khan, I., Khan, S., Zhang, Y., Zhou, J., 2021. Genome-wide analysis and functional characterization of the dof transcription factor family in rice (*Oryza sativa* L.). Planta 253, 101. https://doi.org/10.1007/s00425-021-03627-y.
Kojonna, T., Suttiyut, T., Khunpolwattana, N., Pongpanich, M., Suriya-arunroj, D., Comai, L., Buaboocha, T., Chadchawan, S., 2022. Identification of a negative regulator for salt tolerance at seedling stage via a genome-wide association study of Thai Rice populations. Int. J. Mol. Sci. 23 https://doi.org/10.3390/ijms23031842.
Kushwaha, H., Gupta, S., Singh, V.K., Rastogi, S., Yadav, D., 2011. Genome wide identification of dof transcription factor gene family in sorghum and its comparative phylogenetic analysis with rice and *Arabidopsis*. Mol. Biol. Rep. 38, 5037–5053. https://doi.org/10.1007/s11033-010-0650-9.
Lai, X., Vega-Léon, R., Hugouvieux, V., Blanc-Mathieu, R., van der Wal, F., Lucas, J., Silva, C.S., Jourdain, A., Muino, J.M., Nanao, M., Immink, H., Kaufmann, R., Parcy, K., Smaczniak, F., Zubieta, C, C., 2021. The intervening domain is required for DNA-binding and functional identity of plant MADS transcription factors. Nat. Commun. 12, 4760. https://doi.org/10.1038/s41467-021-24978-w.
Le Hir, R., Bellini, C., 2013. The plant-specific dof transcription factors family: new players involved in vascular system development and functioning in *Arabidopsis*. Front. Plant Sci. 4, 164. https://doi.org/10.3389/fpls.2013.00164.
Li, D., Yang, C., Li, X., Gan, Q., Zhao, X., Zhu, L., 2009. Functional characterization of rice OsDof12. Planta 229, 1159–1169. https://doi.org/10.1007/s00425-009-0893-7.
Li, H., Huang, W., Liu, Z.W., Wang, Y.X., Zhuang, J., 2016. Transcriptome-based analysis of dof family transcription factors and their responses to abiotic stress in tea plant (*Camellia sinensis*). Int. J. Genom. 2016, 5614142 https://doi.org/10.1155/2016/5614142.
Li, N., Yang, R., Shen, S., Zhao, J., 2024. Molecular mechanism of flowering time regulation in *Brassica rapa*: Similarities and differences with *Arabidopsis*. Hortic. Plant J. https://doi.org/10.1016/j.hpj.2023.05.020.
Li, X., Han, S., Wang, G., Liu, X., Amombo, E., Xie, Y., Fu, J., 2017. The fungus *Aspergillus aculeatus* enhances salt-stress tolerance, metabolite accumulation, and improves forage quality in perennial ryegrass. Front. Microbiol. 8, 1664. https://doi.org/10.3389/fmicb.2017.01664.
Lijavetzky, D., Carbonero, P., Vicente-Carbajosa, J., 2003. Genome-wide comparative phylogenetic analysis of the rice and *Arabidopsis Dof* gene families. BMC Evol. Biol. 3, 17. https://doi.org/10.1186/1471-2148-3-17.
Liu, J., Cheng, Z., Xie, L., Li, X., Gao, J., 2019. Multifaceted role of PheDof12-1 in the regulation of flowering time and abiotic stress responses in moso bamboo (*Phyllostachys edulis*). Int. J. Mol. Sci. 20, 424. https://doi.org/10.3390/ijms20020424.
Liu, J., Meng, Q., Xiang, H., Shi, F., Ma, L., Li, Y., Liu, C., Liu, Y., Su, B., 2021. Genome-wide analysis of dof transcription factors and their response to cold stress in rice (*Oryza sativa* L.). BMC Genom. 22, 800. https://doi.org/10.1186/s12864-021-08104-0.
Livak, K.J., Schmittgen, T.D., 2001. Analysis of relative gene expression data using real-time quantitative PCR and the $2^{-\Delta\Delta C(T)}$ method. Methods 25, 402–408. https://doi.org/10.1006/meth.2001.1262.
Ma, J., Li, M.Y., Wang, F., Tang, J., Xiong, A.S., 2015. Genome-wide analysis of dof family transcription factors and their responses to abiotic stresses in Chinese cabbage. BMC Genom. 16, 33. https://doi.org/10.1186/s12864-015-1242-9.
Meena, K.K., Sorty, A.M., Bitla, U.M., Choudhary, K., Gupta, P., Pareek, A., Singh, D.P., Prabha, R., Sahu, P.K., Gupta, V.K., Singh, H.B., Krishanani, K.K., Minhas, P.S., 2017. Abiotic stress responses and microbe-mediated mitigation in plants: the omics strategies. Front. Plant Sci. 8, 172. https://doi.org/10.3389/fpls.2017.00172.
Muthuramalingam, P., Jeyasri, R., Rakkammal, K., Satish, L., Shamili, S., Karthikeyan, A., Valliammai, A., Priya, A., Selvaraj, A., Gowri, P., Wu, Q.S., Karutha Pandian, S., Shin, H., Chen, J.T., Baskar, V., Thiruvengadam, M., Akilan, M., Ramesh, M., 2022. Multi-omics and integrative approach towards understanding salinity tolerance in rice: a review. Biology 11, 1022. https://doi.org/10.3390/biology11071022.
Nedjimi, B., 2011. Is salinity tolerance related to osmolytes accumulation in *Lygeum spartum* L. seedlings? J. Saudi Soc. Agric. Sci. 10, 81–87. https://doi.org/10.1016/j.jssas.2011.03.002.
Pandey, P., Irulappan, V., Bagavathiannan, M.V., Senthil-Kumar, M., 2017. Impact of combined abiotic and biotic stresses on plant growth and avenues for crop improvement by exploiting physio-morphological traits. Front. Plant Sci. 8, 537. https://doi.org/10.3389/fpls.2017.00537.
Park, J.R., Kim, E.G., Jang, Y.H., Jan, R., Farooq, M., Ubaidillah, M., Kim, K.M., 2022. Applications of CRISPR/Cas9 as new strategies for short breeding to drought gene in rice. Front. Plant Sci. 13, 850441 https://doi.org/10.3389/fpls.2022.850441.
Qin, H., Wang, J., Chen, X., Wang, F., Peng, P., Zhou, Y., Miao, Y., Zhang, Y., Gao, Y., Qi, Y., Zhou, J., Huang, R., 2019. Rice OsDOF15 contributes to ethylene-inhibited primary root elongation under salt stress. N. Phytol. 223, 798–813. https://doi.org/10.1111/nph.15824.
Ramirez-Parra, E., Perianez-Rodriguez, J., Navarro-Neila, S., Gude, I., Moreno-Risueno, M.A., Del Pozo, J.C., 2017. The transcription factor OBP4 controls root growth and promotes callus formation. N. Phytol. 213, 1787–1801. https://doi.org/10.1111/nph.14315.
Riechmann, J.L., Heard, J., Martin, G., Reuber, L., Jiang, C.-Z., Keddie, J., Adam, L., Pineda, O., Ratcliffe, O.J., Samaha, R.R., Creelman, R., Pilgrim, M., Broun, P., Zhang, J.Z., Ghandehari, D., Sherman, B.K., Yu, G., 2000. *Arabidopsis* transcription factors: genome-wide comparative analysis among eukaryotes. Science 290, 2105–2110. https://doi.org/10.1126/science.290.5499.2105.
Rose, G., Osborne, T., Greatrex, H., Wheeler, T., 2016. Impact of progressive global warming on the global-scale yield of maize and soybean. Clim. Change 134, 417–428. https://doi.org/10.1007/s10584-016-1601-9.
Rymen, B., Kawamura, A., Schäfer, S., Breuer, C., Iwase, A., Shibata, M., Ikeda, M., Mitsuda, N., Koncz, C., Ohme-Takagi, M., Matsui, M., Sugimoto, K., 2017. ABA suppresses root hair growth via the OBP4 transcriptional regulator. Plant Physiol. 173, 1750–1762. https://doi.org/10.1104/pp.16.01945.
Santos, L.A., de Souza, S.R., Fernandes, M.S., 2012. OsDof25 expression alters carbon and nitrogen metabolism in *Arabidopsis* under high N-supply. Plant Biotechnol. Rep. 6, 327–337. https://doi.org/10.1007/s11816-012-0227-2.
Shim, Y., Kang, K., An, G., Paek, N.C., 2019. Rice DNA-binding one zinc finger 24 (OsDOF24) delays leaf senescence in a jasmonate-mediated pathway. Plant Cell Physiol. 60, 2065–2076. https://doi.org/10.1093/pcp/pcz105.
Singh, P., Mahajan, M.M., Singh, N.K., Kumar, D., Kumar, K., 2020. Physiological and molecular response under salinity stress in bread wheat (*Triticum aestivum* L.). J. Plant Biochem. Biotechnol. 29, 125–133. https://doi.org/10.1007/s13562-019-00521-3.
Singh, R.K., Kota, S., Flowers, T.J., 2021. Salt tolerance in rice: seedling and reproductive stage QTL mapping come of age. Theor. Appl. Genet. 134, 3495–3533. https://doi.org/10.1007/s00122-021-03890-3.
Skirycz, A., Reichelt, M., Burow, M., Birkemeyer, C., Rolcik, J., Kopka, J., Zanor, M.I., Gershenzon, J., Strnad, M., Szopa, J., Mueller-Roeber, B., Witt, I., 2006. Dof transcription factor AtDof1.1 (OBP2) is part of a regulatory network controlling glucosinolate biosynthesis in *Arabidopsis*. Plant J. 47, 10–24. https://doi.org/10.1111/j.1365-313X.2006.02767.x.
Skirycz, A., Radziejwoski, A., Busch, W., Hannah, M.A., Czeszejko, J., Kwaśniewski, M., Zanor, M.I., Lohmann, J.U., De Veylder, L., Witt, I., Mueller-Roeber, B., 2008. The dof transcription factor OBP1 is involved in cell cycle regulation in *Arabidopsis thaliana*. Plant J. 56, 779–792. https://doi.org/10.1111/j.1365-313X.2008.03641.x.
Smyth, D.R., 2023. How flower development genes were identified using forward genetic screens in *Arabidopsis thaliana*. Genetics 224, iyad102. https://doi.org/10.1093/genetics/iyad102.
Sonsungsan, P., Chantanakool, P., Suratanee, A., Buaboocha, T., Comai, L., Chadchawan, S., Plaimas, K., 2021. Identification of key genes in 'Luang Pratahn', Thai salt-tolerant rice, based on time-course data and weighted co-expression networks. Front. Plant Sci. 12, 744654 https://doi.org/10.3389/fpls.2021.744654.
Tang, R.J., Wang, C., Li, K., Luan, S., 2020. The CBL-CIPK calcium signaling network: unified paradigm from 20 years of discoveries. Trends Plant Sci. 25, 604–617. https://doi.org/10.1016/j.tplants.2020.01.009.
Verma, V., Ravindran, P., Kumar, P.P., 2016. Plant hormone-mediated regulation of stress responses. BMC Plant Biol. 16, 86. https://doi.org/10.1186/s12870-016-0771-y.
Vidal, E.A., Moyano, T.C., Riveras, E., Contreras-López, O., Gutiérrez, R.A., 2013. Systems approaches map regulatory networks downstream of the auxin receptor AFB3 in the nitrate response of *Arabidopsis thaliana* roots. Proc. Natl. Acad. Sci. U. S. A. 110, 12840–12845. https://doi.org/10.1073/pnas.1310937110.
Wang, H.W., Zhang, B., Hao, Y.J., Huang, J., Tian, A.G., Liao, Y., Zhang, J.S., Chen, S.Y., 2007. The soybean dof-type transcription factor genes, GmDof4 and GmDof11, enhance lipid content in the seeds of transgenic *Arabidopsis* plants. Plant J. 52, 716–729. https://doi.org/10.1111/j.1365-313X.2007.03268.x.
Ward, J.M., Cufr, C.A., Denzel, M.A., Neff, M.M., 2005. The dof transcription factor OBP3 modulates phytochrome and cryptochrome signaling in *Arabidopsis*. Plant Cell 17, 475–485. https://doi.org/10.1105/tpc.104.027722.
Washio, K., 2003. Functional dissections between GAMYB and dof transcription factors suggest a role for protein-protein associations in the gibberellin-mediated expression of the *RAmy1A* gene in the rice aleurone. Plant Physiol. 133, 850–863. https://doi.org/10.1104/pp.103.027334.
Wu, Q., Li, D., Li, D., Liu, X., Zhao, X., Li, X., Li, S., Zhu, L., 2015. Overexpression of OsDof12 affects plant architecture in rice (*Oryza sativa* L.). Front. Plant Sci. 6, 833. https://doi.org/10.3389/fpls.2015.00833.
Xu, P., Cai, W., 2019. Nitrate-responsive OBP4-XTH9 regulatory module controls lateral root development in *Arabidopsis thaliana*. PLOS Genet 15, e1008465. https://doi.org/10.1371/journal.pgen.1008465.
Xu, P., Chen, H., Ying, L., Cai, W., 2016. AtDOF5.4/OBP4, a dof transcription factor gene that negatively regulates cell cycle progression and cell expansion in *Arabidopsis thaliana*. Sci. Rep. 6, 27705 https://doi.org/10.1038/srep27705.

Xu, T., Niu, J., Jiang, Z., 2022. Sensing mechanisms: calcium signaling mediated abiotic stress in plants. Front. Plant Sci. 13, 925863 https://doi.org/10.3389/fpls.2022.925863.

Yamamoto, M.P., Onodera, Y., Touno, S.M., Takaiwa, F., 2006. Synergism between RPBF dof and RISBZ1 bZIP activators in the regulation of rice seed expression genes. Plant Physiol. 141, 1694–1707. https://doi.org/10.1104/pp.106.082826.

Yanagisawa, S., 2004. Dof domain proteins: plant-specific transcription factors associated with diverse phenomena unique to plants. Plant Cell Physiol. 45, 386–391. https://doi.org/10.1093/pcp/pch055.

Yanagisawa, S., Schmidt, R.J., 1999. Diversity and similarity among recognition sequences of dof transcription factors. Plant J. 17, 209–214. https://doi.org/10.1046/j.1365-313x.1999.00363.x.

Yanagisawa, S., Akiyama, A., Kisaka, H., Uchimiya, H., Miwa, T., 2004. Metabolic engineering with Dof1 transcription factor in plants: improved nitrogen assimilation and growth under low-nitrogen conditions. Proc. Natl. Acad. Sci. U. S. A. 101, 7833–7838. https://doi.org/10.1073/pnas.0402267101.

Zhang, B., Chen, W., Foley, R.C., Büttner, M., Singh, K.B., 1995. Interactions between distinct types of DNA binding proteins enhance binding to ocs element promoter sequences. Plant Cell 7, 2241–2252. https://doi.org/10.1105/tpc.7.12.2241.

Zhang, L., Liu, B., Zheng, G., Zhang, A., Li, R., 2017. Genome-wide characterization of the *SiDof* gene family in foxtail millet (*Setaria italica*). Biosystems 151, 27–33. https://doi.org/10.1016/j.biosystems.2016.11.007.

Zhu, J.K., 2016. Abiotic stress signaling and responses in plants. Cell 167, 313–324. https://doi.org/10.1016/j.cell.2016.08.029.